Zener solutions for particle growth in multi-component alloys

F.J. Vermolen

F.J.Vermolen@math.tudelft.nl

Delft Institute for Applied Mathematics,

Delft University of Technology,

Mekelweg 4, 2628 CD Delft, the Netherlands

Abstract

In this paper the Zener theory on precipitate growth in supersaturated alloys for planar, cylindrical and spherical geometries is extended to multi-component alloys. The obtained solutions can be used to check the results from numerical simulations under simplified conditions. Further, the multi-component solutions are used to derive the quasi-binary diffusion coefficient for planar, cylindrical and spherical geometries of the growing particle in a multi-component alloy. In the illustrations, hypothetic data are used.

1 Introduction

In the thermal processing of both ferrous and non-ferrous alloys, homogenization of as-cast microstructure by annealing at such a high temperature that unwanted precipitates are fully dissolved, is required to obtain a microstructure suited to undergo heavy plastic deformation. Such a homogenization treatment is applied to hot-rolling of Al killed construction steels, HSLA steels, all engineering steels, as well as aluminum extrusion alloys. Next to precipitate dissolution, which is often the most critical of the occurring processes, particles nucleate and grow from a supersaturated solution. The minimum temperature at which the annealing should take place can be determined from thermodynamic analysis of the phases present. Another important quantity is the minimum annealing time at this

annealing temperature. This time, however, is not a constant but depends on particle size, particle concentration, overall concentration, *etc.*

Due to the scientific and the industrial relevance of being able to predict the kinetics of particle dissolution and growth, many models of various complexity have been presented and experimentally validated. The early models on particle dissolution and growth based on long-distance diffusion consisted of analytic solutions in an unbounded medium under the assumption of local equilibrium at the interface, see Ham [1, 2], Zener [3], Whelan [4] and Aaron and Kotler [5] to mention a few. The model of Nolfi *et al.* [6] incorporates the interfacial reaction between the dissolving particle and its surrounding phase. Later modeling particle dissolution and growth has been extended to the introduction of multi-component particles by, among others, Anderson and Ågren [7], Ågren [8], Ågren and Vassilev [9], Thornton *et al.* [10], Reiso *et al.* [11], Hubert [12], Vitek *et al.* [13], Vusanovic and Krane [14], Atkinson *et al.* [15] and Vermolen *et al.* [16, 17]. In these papers particle dissolution and growth was viewed as a Stefan problem with a sharp interface separating the adjacent phases. Several numerical methods exist to solve Stefan problems related to particle dissolution and growth and to solidification or melting problems. A survey on numerical methods is given by Crank [18]. The most commonly used methods are the fixed grid and moving grid methods. Segal *et al.* [19] extended the moving grid method introduced for the Stefan problem by Murray & Landis [20] to a two-dimensional finite element framework. A state-of-the-art fixed grid method is the level set method introduced by Osher & Sethian [21]. The method was described later in a general way by Sethian [22] and by Osher & Fedkiw [23]. It was firstly applied to a Stefan problem with two spatial dimensions by Chen *et al.* [24]. A comparative study between the level set method, moving grid method and phase field method is due to Javierre *et al.* [25] and Kovačević & Šarler [26]. In a parallel study the level set method is applied for three spatial coordinates by Javierre *et al.* [27]. Further, there the method is extended to a vector valued Stefan problem for a multi-component alloy.

Thornton *et al.* [10] present an extensive review paper on the various models for precipitate dissolution and growth. In that paper, next to viewing particle dissolution and

growth as a Stefan problem with a sharp interface, also diffuse-interface models, such as the phase-field method, the Cahn-Hilliard equation, are presented with the appropriate references for the metallurgical literature.

In this study we describe particle growth as a Stefan problem, *i.e.* a diffusion equation with a moving sharp interface interface between the particle and its surrounding diffusive phase. We assume that the particle is allowed to grow in an infinite alloy, which enables us to get exact analytic solutions for a planar, cylindrical and spherical particle. The solutions that we develop have been presented in a different way by Zener [3]. It is our aim to extend these solutions to a multi-component alloy. This has not yet been done for these three geometries, as far as we know. Further, we apply the extension of the Zener solutions to get hold of a quasi-binary diffusion coefficient for planar, cylindrical and spherical geometries. For the planar case, this was done earlier in [28] under approximations. As far as known to the author, this has not yet been extended to other geometries, which is done in the present paper.

2 The mathematical problem

The as-cast microstructure is simplified into a representative cell containing a stoichiometric β particle with a given shape surrounded by an α diffusive phase in which the alloying element diffuses. Both a uniform and spatially varying initial concentration at $t = 0$ can be dealt with in the model. The boundary between the particle and diffusive phase is referred to as the interface. Particle growth is assumed to proceed via the following steps: decomposition of the particle, crossing of the interface by the atoms from the particle and finally long-distance diffusion of the atoms in the diffusive phase. In the present paper long-distance diffusion is assumed to control the interface motion, i.e. local thermodynamic equilibrium is assumed at the interface and hence the interface concentration is the concentration as predicted by the thermodynamic phase diagram at the annealing temperature. Further, it is assumed that the particle concentration is constant all over the particle and at all stages of the dissolution process.

The interface, consisting of a point, curve or a surface for respectively a one-, two- or three-dimensional domain of computation, is denoted by $S = S(t)$. In the present similarity solutions the effects of soft-impingement are neglected, i.e. the interparticle distance is assumed to be very large. This is an inaccurate approximation if the overall composition is large, i.e. the interparticle distance is relatively small. It is known that the nucleation stage should be modelled by approaches that totally differ from the moving boundary problem until the particle reaches the size of the critical nucleus. An example of such methods is the model of heterogeneous nucleation due to Myhr & Grong [29]. Further, the domain of computation is split into the diffusive part (the α-diffusive phase), denoted by $\Omega = \{x \in \mathbb{R} : x > S(t)\}$ and the β-particle $\Omega_p = \{x \in \mathbb{R} : 0 < x < S(t)\}$. First, the binary problem is posed. Subsequently the multi-component model is described.

2.1 The binary model

The distribution of the alloying element is determined by diffusion in the diffusive phase Ω, which gives

$$\frac{\partial c}{\partial t} = D\Delta c = D\left\{\frac{\partial^2 c}{\partial r} + \frac{a}{r}\frac{\partial c}{\partial r}\right\}, \text{ for } r \in \Omega \text{ and } t > 0. \tag{1}$$

Here D represents the diffusion coefficient and r denotes the spatial position within the domain of computation. Further, $a = 0$, $a = 1$, $a = 2$ respectively correspond to planar, cylindrical and spherical symmetry. In the present study D is treated as a constant. Within the particle the concentration is equal to a given constant, hence

$$c = c^{\text{part}}, \text{ for } r \in \Omega_p \text{ and } t \geq 0. \tag{2}$$

On the interface, $S(t)$, local equilibrium is assumed, i.e. the concentration is as predicted by the thermodynamic phase diagram, i.e.

$$\lim_{r \to S^+(t)} c = c^{\text{sol}}, \text{ for } t > 0. \tag{3}$$

The initial concentration is denoted by c^0. Further, it is assumed that the concentration did not change at infinity, i.e.

$$\lim_{r \to \infty} c = c^0, \text{ for } t > 0. \tag{4}$$

Since the concentration satisfies a maximum principle, the above relation implies a horizontal asymptote at infinity. From a mass balance, the equation of motion of the interface can be derived, this equation is commonly referred to as the Stefan condition, and is given by:

$$(c^{\text{part}} - c^{\text{sol}})S'(t) = D \lim_{r \to S^+(t)} \frac{\partial c}{\partial r}, \text{ for } t > 0. \tag{5}$$

Here $S'(t)$ represents the interface velocity. The problem is completed with the initial concentration c^0 and the initial position of the interface $S(0) = 0$, i.e. there is no particle initially. The problem, consisting of equations (1), (2), (3), (4) and (5), is referred to as a Stefan problem for particle dissolution or particle growth.

For the above presented problem Zener-type analytic solutions for various geometries are obtained using the Boltzmann transformation.

2.2 The multi-component model

Now the same definitions for geometry as in the previous section are used. However, now the simultaneous diffusion of several alloying elements is considered. Let n_S be the total number of chemical elements that are considered, then, we have for each alloying element i:

$$\frac{\partial c_i}{\partial t} = D_i \Delta c_i = D_i \left\{ \frac{\partial^2 c_i}{\partial r} + \frac{a}{r} \frac{\partial c_i}{\partial r} \right\}, \text{ for } r \in \Omega \text{ and } t > 0. \tag{6}$$

It is noted that the effects of cross-diffusion can be dealt with in an analogous manner if the diffusion matrix is diagonalizable. This is not treated in more detail in the present study. The particle concentration is treated as constant as before, i.e. for each chemical element i:

$$c_i = c_i^{\text{part}}, \text{ for } r \in \Omega_p \text{ and } t \geq 0. \tag{7}$$

On the interface, local equilibrium is assumed, hence the interface concentrations are determined by the phase diagram following from thermodynamics, that is

$$F(c_1^S, \ldots, c_{n_S}^S) = 0, \tag{8}$$

where $c_i^S := \lim_{r \to S^+(t)} c_i$. In the ideal stoichiometric case, the above relation is hyperbolic, resulting into

$$(c_1^S)^{m_1} (\ldots)(c_{n_S}^S)^{m_{n_S}} = K. \tag{9}$$

To keep things general, the above function F is assumed to be known. Similarly as in the binary model, the initial concentration is known and denoted by c_i^0 for all chemical elements, and hence at infinity we have for each chemical element i:

$$\lim_{r \to \infty} c_i = c_i^0, \text{ for } t > 0. \tag{10}$$

From a mass balance, the equation of motion of the interface can be derived, therewith we get for each alloying element i:

$$(c_i^{\text{part}} - c_i^S)S'(t) = \lim_{r \to S^+(t)} D_i \frac{\partial c_i}{\partial r}, \text{ for } t > 0. \tag{11}$$

From the above set of equations, the interface concentrations, concentration profiles in Ω and interface velocity and position are obtained. First, the interface velocity can be eliminated since the above equation (11) has to hold for each alloying element. This gives

$$\frac{1}{c_i^{\text{part}} - c_i^S} \lim_{r \to S^+(t)} D_i \frac{\partial c_i}{\partial r} = \frac{1}{c_j^{\text{part}} - c_j^S} \lim_{r \to S^+(t)} D_j \frac{\partial c_j}{\partial r}, \text{ for each } i \neq j. \text{ for } t > 0. \tag{12}$$

The above problem is solved in Section 3.2.

3 Analytic solutions

First the analytic solutions for the binary case, which are the backbone for the multi-component case, are considered. Subsequently, this analytic solution is extended to multi-component alloys.

3.1 Solutions for the binary model

As an 'Ansatz' solutions in the form of $c(r,t) = u(x)$, where $x := \dfrac{r}{\sqrt{t}}$ are tried. Then, one obtains after substitution into equation (1) and subsequent multiplication by t:

$$-\frac{x}{2}u'(x) = D\{u''(x) + \frac{a}{x}u'(x)\}. \tag{13}$$

Further, for the interface position, $S(t)$, one tries $S(t) = k\sqrt{t}$. Solution of equation (13) gives after using an integrating factor and integration twice:

$$u(x) = C_1 \int_k^x \frac{1}{z^a}\exp\left(-\frac{z^2}{4D}\right)dz + C_2. \tag{14}$$

From the above relation, it is clear that $a = 0$ (the planar case) gives the ordinary complementary error function. The 'boundary conditions' are

$$\lim_{x \to k^+} u = c^{\text{sol}}, \text{ and } \lim_{x \to \infty} u = c^0. \tag{15}$$

This implies for the constants of integration C_1 and C_2:

$$C_1 = \frac{c^0 - c^{\text{sol}}}{\int_k^\infty \frac{1}{x^a}\exp\left(-\frac{x^2}{4D}\right)dx}, \quad C_2 = c^{\text{sol}}. \tag{16}$$

Hence the solution for $x > k$ is given by

$$u(x) = \frac{c^0 - c^{\text{sol}}}{\int_k^\infty \frac{1}{z^a}\exp\left(-\frac{z^2}{4D}\right)dz} \int_k^x \frac{1}{z^a}\exp\left(-\frac{z^2}{4D}\right)dz + c^{\text{sol}}. \tag{17}$$

The equation of motion (5) is used to determine the value of k

$$\frac{dS}{dt} = \frac{k}{2\sqrt{t}} = \frac{D}{c^{\text{part}} - c^{\text{sol}}}\frac{u'(k)}{\sqrt{t}}. \tag{18}$$

Differentiation of equation (17) and substitution of the result into equation (18) gives the following transcedental equation for k

$$\frac{k}{2} = \frac{D}{c^{\text{part}} - c^{\text{sol}}} \cdot \frac{c^0 - c^{\text{sol}}}{\int_k^\infty \frac{1}{z^a}\exp\left(-\frac{z^2}{4D}\right)dz} \cdot \frac{\exp\left(-\frac{k^2}{4D}\right)}{k^a}. \tag{19}$$

In the above expression the integral has to be evaluated for the various values of a, that is for the various geometries. Therefore, the integral I_a is defined by

$$I_a := \int_k^\infty \frac{1}{z^a} \exp\left(-\frac{z^2}{4D}\right) dz. \tag{20}$$

First, by substitution of $y := \frac{x}{2\sqrt{D}}$, one obtains

$$I_a = \frac{1}{(2\sqrt{D})^{a-1}} \int_{\frac{k}{2\sqrt{D}}}^\infty \frac{e^{-y^2}}{y^a} dy. \tag{21}$$

Now the cases $a = 0$, $a = 1$ and $a = 2$ are treated consecutively. For $a = 0$, which is the planar particle, this gives

$$I_0 = 2\sqrt{D} \int_{\frac{k}{2\sqrt{D}}}^\infty e^{-y^2} dy = \sqrt{\pi D}\,\mathrm{erfc}\left(\frac{k}{2\sqrt{D}}\right), \tag{22}$$

which is the familiar result for particle growth. For $a = 1$, which is the cylindrical particle, one obtains

$$I_1 = \int_{\frac{k}{2\sqrt{D}}}^\infty \frac{e^{-y^2}}{y} dy = \frac{1}{2} \int_{\frac{k^2}{4D}}^\infty \frac{e^{-u}}{u} du = \frac{1}{2} Ei\left(\frac{k^2}{4D}\right), \tag{23}$$

which is the exponential integral. Finally for $a = 2$, which is the spherical particle, this yields

$$I_2 = \frac{1}{2\sqrt{D}} \int_{\frac{k}{2\sqrt{D}}}^\infty \frac{e^{-y^2}}{y^2} dy = \frac{e^{-\frac{k^2}{4D}}}{k} - \frac{1}{2}\sqrt{\frac{\pi}{D}}\,\mathrm{erfc}\left(\frac{k}{2\sqrt{D}}\right). \tag{24}$$

These expressions (22), (23) and (24) are substituted into equation (19) and, then, a solution for the interface velocity parameter k is obtained after a zero-point method. The above integrals can be classified as gamma-functions. The solutions that have been derived here are classical Zener solutions. The main innovation in the present work is the extension to multi-component solutions, which is described in the next section.

3.2   Solutions for the multi-component model

The solution is similar as in the previous section. Since the result of the interface velocity must be the same for all chemical species, we have for all $i \in \{1, \ldots, n_S\}$

$$\frac{k}{2} = \frac{D_i}{c_1^{\mathrm{part}} - c_i^S} \cdot \frac{c_i^0 - c_i^S}{\int_k^\infty \frac{1}{z^a} \exp\left(-\frac{z^2}{4D_i}\right) dz} \cdot \frac{e^{-\frac{k^2}{4D_i}}}{k^a}. \tag{25}$$
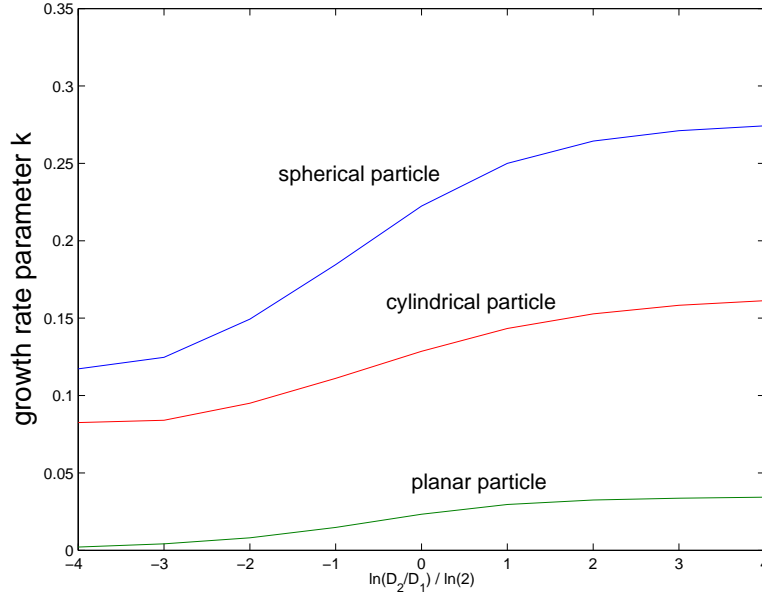
Figure 1: The growth rate parameter k as a function of the logarithm of the ratio of the diffusivities for a spherical, cylindrical and spherical particle.

Next to the above equation, equation (8) holds. Hence equations (8) and (25) constitute a system of algebraic equations to be solved for c_i^S and interface velocity parameter k. Note that for $a = 0$ the planar solution as in [28] is retrieved. Note further that equations (22), (23) and (24) can be substituted into the integral in the above equation to be solved by a zero-point method for a system of algebraic equations.

3.3   Applications

3.3.1   The influence of the ratio $\frac{D_1}{D_2}$

As a basic configuration a hypothetic case with

$$c_1^{\text{part}} = 50 = c_2^{\text{part}}, \quad c_1^0 = 2 = c_2^0, \quad D_1 = 1, \quad c_1^S c_2^S = K = 1, \tag{26}$$

is dealt with. Here the diffusion coefficient of the second alloying element is varied for the several geometries. The results have been plotted in Figure 1 where k is displayed as a function of D_2 for the three geometries. From Figure 1 it is clear that also in the multi-

component case the spherical particles grow fastest and that the planar is the slowest. Further, from Figure 1 it can be seen that for $D_2 \to 0$ and $D_2 \to \infty$ the derivative of the dissolution speed with respect to D_2 becomes smaller. This holds for all cases.

3.3.2 The quasi-binary diffusion coefficient

Suppose that the rate parameter k is known for a certain configuration. Now, the aim is to find the quasi-binary diffusion coefficient, which is the diffusion coefficient that holds identically for each alloying element, such that the growth rate is the same. For this purpose, equation (25) has to be solved for a given geometry. For this case, k is known and D is the unknown, for which $D_1 = \ldots = D_{n_S} = D$, which is the quasi-binary diffusion coefficient. In this application, the interface concentrations $c_1^S, \ldots, c_{n_S}^S$ and the quasi-binary diffusion coefficient have to be determined. Suppose that we have the same configuration as in the previous case (26), with $D_1 = 1$ and $D_2 = 1/2^4 = 0.0625$, then we obtain for the planar particle a rate parameter $k = 0.00811536$. This would give an quasi-binary diffusion coefficient $D = 0.1209780 = 1/2^{3.0471}$. For the cylindrical and spherical cases, the results have been presented in Table 1.

Table 1: Rate coefficients and quasi-binary diffusivities for several geometries

parameter	planar	cylindrical	spherical
k	$8.11536 \cdot 10^{-3}$	$9.501586 \cdot 10^{-2}$	0.14936582
D	$0.1209780 = 1/2^{3.0471}$	$0.1848582 = 1/2^{2.436}$	$0.158058085 = 1/2^{2.6615}$

It is noted here that the interface concentrations are both equal to one due to equality of the particle concentrations, initial concentrations and the diffusion coefficients. From the above data it can be seen that the quasi-binary diffusion coefficient depends on geometry but lies somewhere between the two diffusion coefficients but closer to the lowest value. This depends on the ratio of the particle concentrations. We further note that the quasi-binary diffusion coefficients derived in [28] only hold for the planar case and under the approximation that the initial concentration is zero. Here, for the growth case this would be a bad approximation since the initial concentration is larger than the interface

concentrations here.

4   Discussion

Since metallic alloys often contain secondary particles in the form of plates, needles and spherical particles, analytic solutions for several geometries have been constructed for the growth of particles. These particles grow as a result from nucleation and diffusion. The earliest nucleation stage proceeds by steps that cannot be dealt with by the present model since the particle has to grow larger than a critical nucleus size due to the surface tension effects. This process is modelled in the nucleation models, such as the heterogeneous model due to Myhr and Grong [29], in the Avrami-style models, or in the spirit of Monte-Carlo simulations. The present solutions neglect this behaviour and are constructed as a mathematical exercise that can be used to calibrate the results of numerical models for the case that the Gibbs-Thomson effect and nucleation issues have been disregarded. Nevertheless the present solutions can be used to gain insight into the influence of the geometry of the growing particle, such as that the spherical particles grow faster than the cylindrical- and planar particles. The planar particles grow slowest. These results are of course for the case that the Gibbs-Thomson effect has been disregarded. The paper should be considered in the spirit of the existing Zener nucleation models where an extension has been made to a vector Stefan problem for particle growth in a multi-component alloy. The case of dissolution of a planar particle can be tackled similarly. For the dissolution of spherical and cylindrical (needle-shaped) particles one can use approximate analytic solutions.

5   Conclusions

Analytic solutions for particle growth in one, two and three dimensions with rotational symmetry are presented and evaluated. It is found that the spherical particles grow fastest, whereas the planar particles are slowest. The solutions obtained can be used as test-cases

to validate solutions obtained from numerical procedures such as moving grid or level-set methods. Further, the solutions can be used to determine the quasi-binary diffusion coefficients for the various geometries. From the study, it has turned out that the quasi-binary diffusion coefficient depends on the geometry of the growing particle. We bear in mind that the here presented solutions do not reflect reality well since the nucleation part of growth should be modelled by the use of completely different principles. Furthermore, the surface tension, i.e. the Gibbs-Thomson effect, has a significant effect during the early stages of particle growth.

References

[1] F.S. Ham. Theory of diffusion-limited growth. *Journal of Physics and Chemistry in Solids*, 6:335–351, 1958.

[2] F.S. Ham. Stress-assisted precipitation on dislocations. *Journal of Applied Physics*, 30 (6):915–926, 1958.

[3] C. Zener. Theory of growth of spherical precipitates from solid solution. *Journal of Applied Physics*, 20:950–953, 1949.

[4] M.J. Whelan. On the kinetics of particle dissolution. *Metals Science Journal*, 3:95–97, 1969.

[5] H.B. Aaron and G.R. Kotler. Second phase dissolution. *Metallurgical Transactions*, 2:1651–1656, 1971.

[6] F.V. Nolfi jr., P.G. Shewmon, and J.S. Foster. The dissolution and growth kinetics of spherical particles. *Transactions of the Metallurgical Society of AIME*, 245:1427–1433, 1969.

[7] J.-O. Andersson and J. Ågren. Models for numerical treatment of multicomponent diffusion in simple phases. *Journal of Applied Physics*, 72 (4):1350–1355, 1981.

[8] J. Ågren. Numerical treatment of diffusional reactions in multi-component alloys. *Journal of Physics and Chemistry of Solids*, 43 (4):285–391, 1982.

[9] J. Ågren and G.P. Vassilev. Computer simulations of cementite dissolution in austenite. *Materials Science and Engineering*, 64:95–103, 1984.

[10] K. Thornton, J. Ågren, and P.W. Voorhees. Modelling the evolution of phase boundaries in solids at the meso- and nano-scales. *Acta Materialia*, 51:5675–5710, 2003.

[11] O. Reiso, N. Ryum, and J. Strid. Melting and dissolution of secondary phase particles in AlMgSi-alloys. *Metallurgical Transactions A*, 24A:2629–2641, 1993.

[12] R. Hubert. Modelisation numerique de la croissance et de la dissolution des precipites dans l'acier. *ATB Metallurgie*, 34-35:4–14, 1995.

[13] J.M. Vitek, S.A. Vitek, and S.A. David. Modelling of diffusion controlled phase transformation in ternary systems and application to the ferrite-austenite transformation in the Fe-Cr-Ni-system. *Metallurgical Transactions A*, 26A:2007–2025, 1995.

[14] I. Vusanovic and M.J. Krane. Microsegregation during solidification of Al-Cu-Mg alloys with varying composition. *International Communications in Heat and Mass Transfer*, 29 (3):1037–1046, 2002.

[15] C. Atkinson, T. Akbay, and R.C. Reed. Theory for reaustenization from ferrite-cementite mixtures in Fe-C-X steels. *Acta Metallurgica et Materialia*, 43 (5):2013–2031, 1995.

[16] F.J. Vermolen, C. Vuik, and S. van der Zwaag. Particle dissolution and cross-diffusion in multi-component alloys. *Materials Science and Engineering A*, A347:265–279, 2003.

[17] F.J. Vermolen and C. Vuik. Solution of vector valued stefan problems with cross-diffusion. *Journal of Computational and Applied mathematics*, 176 (1):179–201, 2005.

[18] J. Crank. *Free and moving boundary problems.* Clarendon Press, Oxford, 1984.

[19] A. Segal, C. Vuik, and F.J. Vermolen. A conserving discretisation for the free boundary in a two-dimensional stefan problem. *Journal of Computational Physics*, 141:1–21, 1998.

[20] W.D. Murray and F. Landis. Numerical and machine solutions of transient heat conduction problems involving freezing and melting. *Transactions ASME (C), Journal of Heat Transfer*, 245:106–112, 1959.

[21] S. Osher and J.A. Sethian. Fronts propagating with curvature-dependent speed: Algorithms based on hamilton-jacobi formulations. *Journal of Computational Physics*, 141:12–49, 1988.

[22] J.A. Sethian. *Level-Set methods and fast marching methods*. Cambridge University Press, New York, 1999.

[23] S. Osher and R. Fedkiw. *Level-Set methods and dynamic implicit surfaces*. Springer-Verlag, New York, 2003.

[24] S. Chen, B. Merriman, S. Osher, and P. Smereka. A simple Level-Set method for solving Stefan problems. *Journal of Computational Physics*, 135:8–29, 1997.

[25] E. Javierre, C. Vuik, F.J. Vermolen, and S. van der Zwaag. A comparison of numerical models for one-dimensional stefan problems. *Journal of Computational and Applied Mathematics*, page accepted, 2005.

[26] I. Kovačević and B. Šarler. Solution of a phase-field model for dissolution of primary particles. *Conference of Advances of Solidification Processes in Stockholm*, 2005.

[27] E. Javierre, C. Vuik, F.J. Vermolen, and A. Segal. A Level Set Method for Particle Dissolution in a Binary Alloy. *in progress*, 2005.

[28] F.J. Vermolen, C. Vuik, and S. van der Zwaag. Cross-diffusion controlled particle dissolution in metallic alloys. *Computing and Visualization in Science*, 8:27–33, 2005.

[29] O.R. Myhr and Ø. Grong. Modelling of non-isothermal transformations in alloys containing a particle distribution. *Acta Materialia*, 48:1605–1615, 2000.